The Astrophysical Journal, 889:62 (8pp), 2020 January 20 https://doi.org/10.3847/1538-4357/ab63ce
© 2020. The American Astronomical Society. All rights reserved.

Evolution of the Deterministic Collapse Barrier of the Field Clusters as a Probe of Cosmology

Suho Ryu and Jounghun Lee
Astronomy program, Department of Physics and Astronomy, Seoul National University, Seoul 08826, Republic of Korea; jmhera2007@snu.ac.kr, jounghun@astro.snu.ac.kr
Received 2019 October 16; revised 2019 December 1; accepted 2019 December 17; published 2020 January 27

Abstract

The collapse barrier, δ_c, of the field clusters located in the low-density environment is deterministic rather than diffusive, unlike that of the wall counterparts located in the superclusters. Analyzing the data from the Mira-Titan simulations for 11 different cosmologies, including the standard ΛCDM cosmology at various redshifts, we investigate the evolution of the deterministic collapse barrier of the field clusters and explore its dependence on the background cosmology. Regardless of the background cosmology, the deterministic δ_c exhibits a universal behavior of having a higher value than the Einstein–de Sitter spherical collapse barrier height of $\delta_{\rm sc} = 1.686$, at $z = 0$, but gradually converging down to $\delta_{\rm sc}$ as the dominance of dark energy diminishes with the increment of z. A significant difference among different cosmologies, however, is found in its convergence rate, as well as in the critical redshift z_c, at which $\delta_c = \delta_{\rm sc}$. Showing that the convergence rate and critical redshifts can distinguish even between the degenerate cosmologies, which yield almost identical linear growth factor and cluster mass functions, we suggest that the evolution of the deterministic collapse barrier of the field clusters should be a powerful complementary probe of cosmology.

Unified Astronomy Thesaurus concepts: Large-scale structure of the universe (902); Cosmological models (337)

1. Introduction

Ever since Press & Schechter (1974) derived an analytic formula for the cluster mass function based on the excursion set theory, its power and usefulness as a cosmological probe has been widely demonstrated and well appreciated in the field of the large-scale structure (e.g., Fan et al. 1997; Wang & Steinhardt 1998; Vikhlinin et al. 2009; Basilakos et al. 2010; Ichiki & Takada 2012; Benson et al. 2013; Planck Collaboration et al. 2014). The excursion set theory basically depicts the gravitational growth and collapse of an overdense region into a bound object as a *random walk process* confined under a barrier whose height is determined by the underlying dynamics. In the original formulation of Press & Schechter (1974), who adopted the spherical dynamics, the height of the collapse barrier has a constant value, $\delta_{\rm sc}$, being independent of the cluster mass. Various *N*-body experiments, however, revealed that the original Press–Schechter mass function failed to match well the numerical results at quantitative levels, implying the inadequacy of the spherical dynamics (Bond & Myers 1996 and references therein).

In the subsequent works, which employed more realistic ellipsoidal dynamics to analytically derive the excursion set mass function, the height of the collapse barrier was deemed no longer a constant value, but a decreasing function of the cluster mass, M, to account for the fact that the collapse process deviates further from the spherical dynamics on the lower-mass scales (e.g., Bond & Myers 1996; Chiueh & Lee 2001; Sheth et al. 2001; Sheth & Tormen 2002). Although better agreements with the numerical results were achieved by employing the mass-dependent ellipsoidal collapse barrier, the purely analytic evaluation of the cluster mass function had to be relinquished, on the ground that no unique condition for the ellipsoidal collapse exists unlike the case of the spherical collapse (Bond & Myers 1996; Chiueh & Lee 2001; Sheth et al. 2001). It was required to empirically determine the functional form of the ellipsoidal collapse barrier height by fitting the analytic formula to the numerical results, which in turn inevitably weakened the power of the cluster mass function as a probe of cosmology. Besides, the high-resolution *N*-body simulations revealed that even on the fixed mass scale the collapse barrier height exhibited substantial variations with the environments as well as with the cluster identification algorithms (e.g., Robertson et al. 2009 and references therein). These numerical findings casted down an excursion set based analytic modeling of the cluster mass function, leading the community to acquiesce in relying on mere fitting formulae with multiple adjustable parameters (e.g., Tinker et al. 2008).

The excursion set modeling of the cluster mass function, however, attracted a revived attention when Maggiore & Riotto (2010a, 2010b) brought up an insightful idea that the collapse barrier height should be treated as a stochastic variable rather than a deterministic value. Ascribing the diffusive scatters of the collapse barrier height to the incessant disturbing influence from the surrounding on the clusters, Maggiore & Riotto (2010a) successfully incorporated the concept of the stochastic barrier height into the excursion set theory with the help of the path integral method and showed that the accuracy of the generalized excursion set mass function with stochastic collapse barrier was considerably improved even though it has only a single parameter, D_B, which measures the degree of the stochasticity of δ_c, whose ensemble average coincides with $\delta_{\rm sc}$.

Corasaniti & Achitouv (2011a, hereafter, CA) derived a more accurate mass function by extending the formalism of Maggiore & Riotto (2010a) to the ellipsoidal collapse case where the ensemble average, $\langle\delta_c\rangle$, does not coincide with $\delta_{\rm sc}$ but drifts away from it, depending on the cluster mass scale. As a tradeoff of introducing an additional parameter, β, to quantify the deviation of $\langle\delta_c\rangle$ from $\delta_{\rm sc}$, Corasaniti & Achitouv (2011a) won two-fold achievement: matching the numerical results as excellently well as pure fitting formula and simultaneously providing much deeper physical understanding about the cluster abundance and its evolution (see also Corasaniti & Achitouv 2011b). Notwithstanding, the efficacy of the generalized excursion set mass

function as a cosmological diagnostics was not greatly elevated by introducing the concept of a *stochastically drifting* collapse barrier due to the obscurity in the choice of the joint probability density functions of δ_c expressed in terms of the two parameters, D_B and β (Achitouv et al. 2014 and references therein).

It was Lee (2012) who fathomed that for the case of the field clusters embedded in the lowest-density environments, the collapse barrier height would behave deterministically (i.e., $D_B = 0$), as the degree of the surrounding disturbance as well as ambiguity in the identification of the field clusters would be negligibly low in the underdense regions. Defining the field clusters as those which do not belong to superclusters, Lee modified the CA formalism by setting $D_B = 0$, and confirmed its validity against the *N*-body results at various redshifts for the case of the currently favored cosmological constant Λ and cold dark matter (ΛCDM) model. The analysis of Lee (2012) also found a clear trend that the value of β gradually dwindles away to 0 as the redshift z increases, which indicates that at some critical redshift, z_c, the deterministic collapse barrier height, δ_c, for the field clusters will become equal to $\delta_{\rm sc}$.

This trend may be physically understood by the following logic. The high-z field clusters correspond to the highest peaks in the linear density field whose gravitational collapse proceeds spherically (Bernardeau 1994). At high redshifts $z > 0.7$ where the dark matter (DM) density exceeds that of dark energy (DE), the universe is well approximated by the Einstein–de Sitter (EdS) cosmology in which $\delta_{\rm sc} = 1.686$ (Gunn & Gott 1972). We speculate that as the convergence rate of the universe to the EdS model is quite susceptible to the background cosmology, the deterministic collapse barrier of the field clusters would evolve differently among different cosmologies. The aim of this paper is to examine if the concept of the deterministic collapse barrier for the field clusters is valid even in *w*CDM (dynamical DE with equation of state w + CDM) cosmologies (Sections 2.1–2.2) and to explore whether or not the evolution of β, i.e., the deviation of the deterministic collapse barrier from the EdS spherical collapse value of $\delta_{\rm sc} = 1.686$, can be used as a complementary probe of cosmology (Section 2.3).

2. Abundance of the Field Clusters in Dark-energy Models

2.1. A Brief Review of the Analytic Model

The excursion set modeling of the cluster mass function relates the differential number density of the clusters, $dN/d\ln M$, to the *multiplicity function*, $f(\sigma)$, as (Reed et al. 2003)

$$\frac{d\,N(M,\,z)}{d\,\ln M} = \frac{\bar{\rho}}{M}\left|\frac{d\,\ln\sigma^{-1}}{d\,\ln M}\right| f[\sigma(M,\,z)], \quad (1)$$

where $\bar{\rho}$ is the mean matter density at the present epoch, and $\sigma(M,\,z)$ is the rms density fluctuation of linear density field smoothed on the mass scale M at redshift z, and $f(\sigma)$ counts the number of the randomly walking overdensities, δ, that just touch the collapse barrier, δ_c, when the underlying linear density field has the inverse of the rms fluctuation in the differential range of $[\ln\sigma^{-1},\,\ln\sigma^{-1} + d\,\ln\sigma^{-1}]$. The cosmology dependence of $dN/d\,\ln M$ stems from the dependence of $\sigma(M,\,z)$ on the linear growth factor, $D(z)$, and linear density power spectrum, $P(k)$ as $\sigma^2(M,\,z) \propto D^2(z)\int_0^\infty dk\,k^2\,P(k)W^2(k,\,M)$ with the spherical top hat window function, $W(k,\,M)$.

Assuming that δ_c is a stochastically drifting variable as in Maggiore & Riotto (2010a, 2010b), the CA formalism approximates the multiplicity function by

$$f_{\rm ca}(\sigma;\,D_B,\,\beta) \approx f^{(0)}(\sigma;\,D_B,\,\beta) + f^{(1)}_{\beta=0}(\sigma;\,D_B) + f^{(1)}_{\beta}(\sigma;\,D_B,\,\beta) + f^{(1)}_{\beta^2}(\sigma;\,D_B,\,\beta), \quad (2)$$

$$f^{(0)}(\sigma;\,D_B,\,\beta) = \frac{\delta_{\rm sc}}{\sigma\sqrt{1+D_B}}\sqrt{\frac{2}{\pi}}\;e^{-\frac{(\delta_{\rm sc}+\beta\sigma^2)^2}{2\sigma^2(1+D_B)}}, \quad (3)$$

$$f^{(1)}_{\beta=0}(\sigma;\,D_B) = -\tilde{\kappa}\frac{\delta_{\rm sc}}{\sigma}\sqrt{\frac{2a}{\pi}}\left[e^{-\frac{a\delta_{\rm sc}^2}{2\sigma^2}} - \frac{1}{2}\Gamma\left(0,\,\frac{a\delta_{\rm sc}^2}{2\sigma^2}\right)\right], \quad (4)$$

$$f^{(1)}_{\beta}(\sigma;\,D_B,\,\beta) = -\beta\,a\,\delta_{\rm sc}\left[f^{(1)}_{\beta=0}(\sigma;\,D_B) + \tilde{\kappa}\,{\rm erfc}\left(\frac{\delta_{\rm sc}}{\sigma}\sqrt{\frac{a}{2}}\right)\right], \quad (5)$$

$$f^{(1)}_{\beta^2}(\sigma;\,D_B,\,\beta) = \beta^2a^2\delta_{\rm sc}^2\tilde{\kappa}\left\{{\rm erfc}\left(\frac{\delta_{\rm sc}}{\sigma}\sqrt{\frac{a}{2}}\right)\right. \quad (6)$$

$$\left. + \frac{\sigma}{a\delta_{\rm sc}}\sqrt{\frac{a}{2\pi}}\left[e^{-\frac{a\delta_{\rm sc}^2}{2\sigma^2}}\left(\frac{1}{2} - \frac{a\delta_{\rm sc}^2}{\sigma^2}\right) + \frac{3}{4}\frac{a\delta_{\rm sc}^2}{\sigma^2}\Gamma\left(0,\,\frac{a\delta_{\rm sc}^2}{2\sigma^2}\right)\right]\right\}, \quad (7)$$

with $a \equiv 1/(1 + D_B)$, $\tilde{\kappa} = \kappa a$, $\kappa = 0.475$, upper incomplete gamma function $\Gamma(0,\,x)$ and complementary error function erfc (x). The statistical properties of the randomly drifting collapse barrier, δ_c, are described by the two parameters, D_B and β, in Equations (2)–(6). The former, called the diffusion coefficient, is related to the scatters of δ_c from its ensemble average, while the latter, called the drifting average coefficient, measures how much the ensemble average of δ_c drifts away from the deterministic height of the spherical collapse barrier $\delta_{\rm sc}$ on a given mass scale (Corasaniti & Achitouv 2011a, 2011b).

Lee (2012) suggested that for the case of the field clusters the collapse barrier height should be deterministic (i.e., $D_B = 0$) rather than stochastic, as the field clusters would experience the least disturbance from the surroundings. Setting $D_B = 0$ in Equation (2) and putting it into Equation (1), Lee modified the CA formalism to evaluate the mass function of the field clusters, $dN_l/d\,\ln M$, as

$$\frac{dN_l(M,\,z)}{d\,\ln M} = \frac{\bar{\rho}}{M}\left|\frac{d\,\ln\sigma^{-1}}{d\,\ln M}\right| f_{\rm ca}[\sigma(M,\,z);\,D_B = 0,\,\beta], \quad (8)$$

which has a single coefficient, β. Empirically determining the values of β at three different redshifts ($z = 0,\,0.5,\,1$) through numerical adjustment process, Lee (2012) confirmed the validity of Equation (8) for the ΛCDM case. In the following subsections, we will test this analytic model against the numerical results from *N*-body simulations performed for various *w*CDM cosmologies and investigate how β evolves in different cosmologies.

2.2. Comparison with the Numerical Results

To investigate if Equation (8) can be validly applied to the case of a *w*CDM cosmology where the DE equation of state, w, evolves with time, we resort to the Mira-Titan simulation conducted by Heitmann et al. (2016) on a periodic box of $(2100\,{\rm Mpc})^3$ with 3200^3 DM particles of individual mass $m_{\rm dm} \sim 10^{10}\,M_\odot$ for 10 different *w*CDM cosmologies (designated

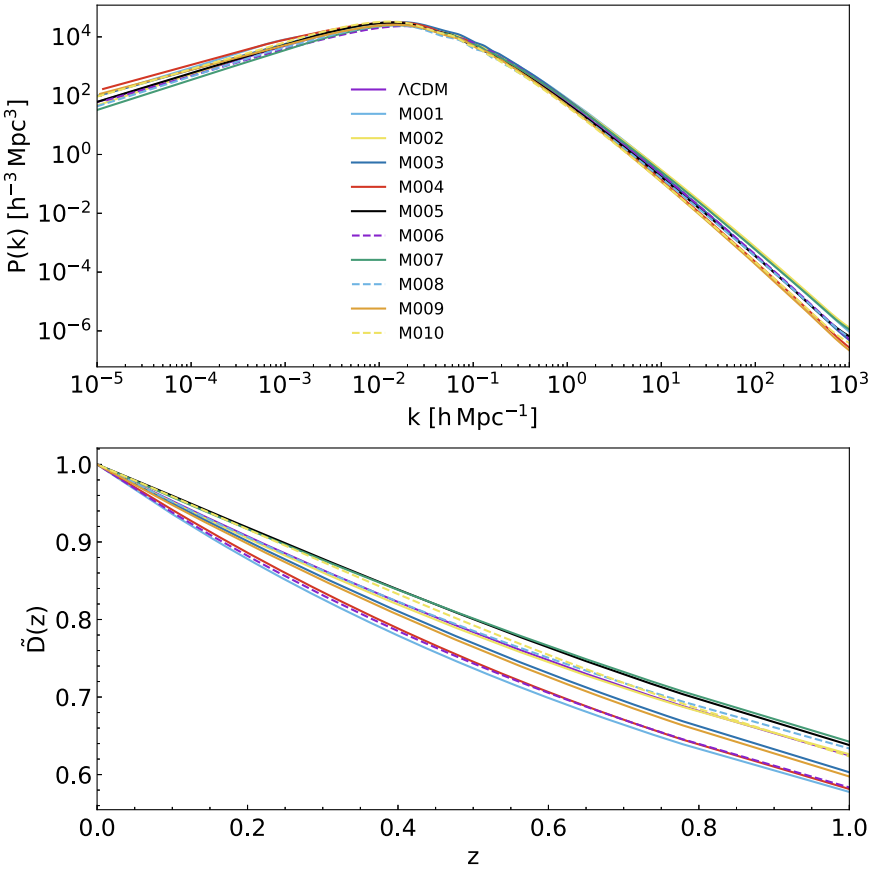

Figure 1. Linear density power spectra (top panel) and linear growth factors (bottom panel) from the Mira-Titan simulations for the cases of the ΛCDM and 10 different dynamical *w*CDM cosmologies (Heitmann et al. 2016).

Table 1
Key Cosmological Parameters for the 11 Models from the HACC Simulations

Cosmology	Ω_m	Ω_b	h	σ_8	n_s	w_0	w_a
ΛCDM	0.2648	0.04479	0.7100	0.8000	0.9630	−1.0000	0.0000
M001	0.3871	0.05945	0.6167	0.8778	0.9611	−0.7000	0.6722
M002	0.2411	0.04139	0.7500	0.8556	1.0500	−1.0330	0.9111
M003	0.3017	0.04271	0.7167	0.9000	0.8944	−1.1000	−0.2833
M004	0.3642	0.06710	0.5833	0.7889	0.8722	−1.1670	1.1500
M005	0.1983	0.03253	0.8500	0.7667	0.9833	−1.2330	−0.0445
M006	0.4354	0.07107	0.5500	0.8333	0.9167	−0.7667	0.1944
M007	0.2265	0.03324	0.8167	0.8111	1.0280	−0.8333	−1.0000
M008	0.2570	0.04939	0.6833	0.7000	1.0060	−0.9000	0.4333
M009	0.3299	0.05141	0.6500	0.7444	0.8500	−0.9667	−0.7611
M010	0.2083	0.03649	0.7833	0.7222	0.9389	−1.3000	−0.5222

as M001, M002, M003, M004, M005, M006, M007, M008, M009, and M010), as well as for the ΛCDM case (see also Habib et al. 2016; Heitmann et al. 2019). The initial condition of each cosmology was specified by seven parameters, $\{\Omega_m, \Omega_b, h, \sigma_8, n_s, w_0$, and $w_a\}$, under the common assumption of a spatially flat geometry ($\Omega_{\rm de} + \Omega_m = 1$), no neutrino ($\Omega_\nu = 0$) and evolution of w given as $w = w_0 + w_a z/(1 + z)$ (Chevallier & Polarski 2001; Linder 2003).

For the ΛCDM case ($w_0 = -1$, $w_a = 0$), the other five cosmological parameters were set at the best-fit values from the Seven-Year *Wilkinson Microwave Anisotropy Probe* (*WMAP*7; (Komatsu et al. 2011). For the *w*CDM cosmologies, the values of the seven key cosmological parameters, including w_0 and w_a, were deliberately chosen to be in the ranges that embrace the *WMAP*7 constraints (for details, see Heitmann et al. 2009, 2016). Table 1 lists the values of the key cosmological parameters for each of the 11 different cosmologies from the Mira-Titan simulation (see also Table 3 in Lawrence et al. 2017). Figure 1 plots the linear power spectra at the present epoch, $P(k)$, and the linear growth factor, $D(z)$, for the 11 cosmologies (in the top and bottom panels, respectively), computed by the CAMB code (Lewis et al. 2000). Note that the three models, M003, M005, and M008 are almost indistinguishable from the ΛCDM model in $P(k)$, while the two models, M007 and M009, yield $D(z)$ the shapes of which are very similar to that for the ΛCDM case.

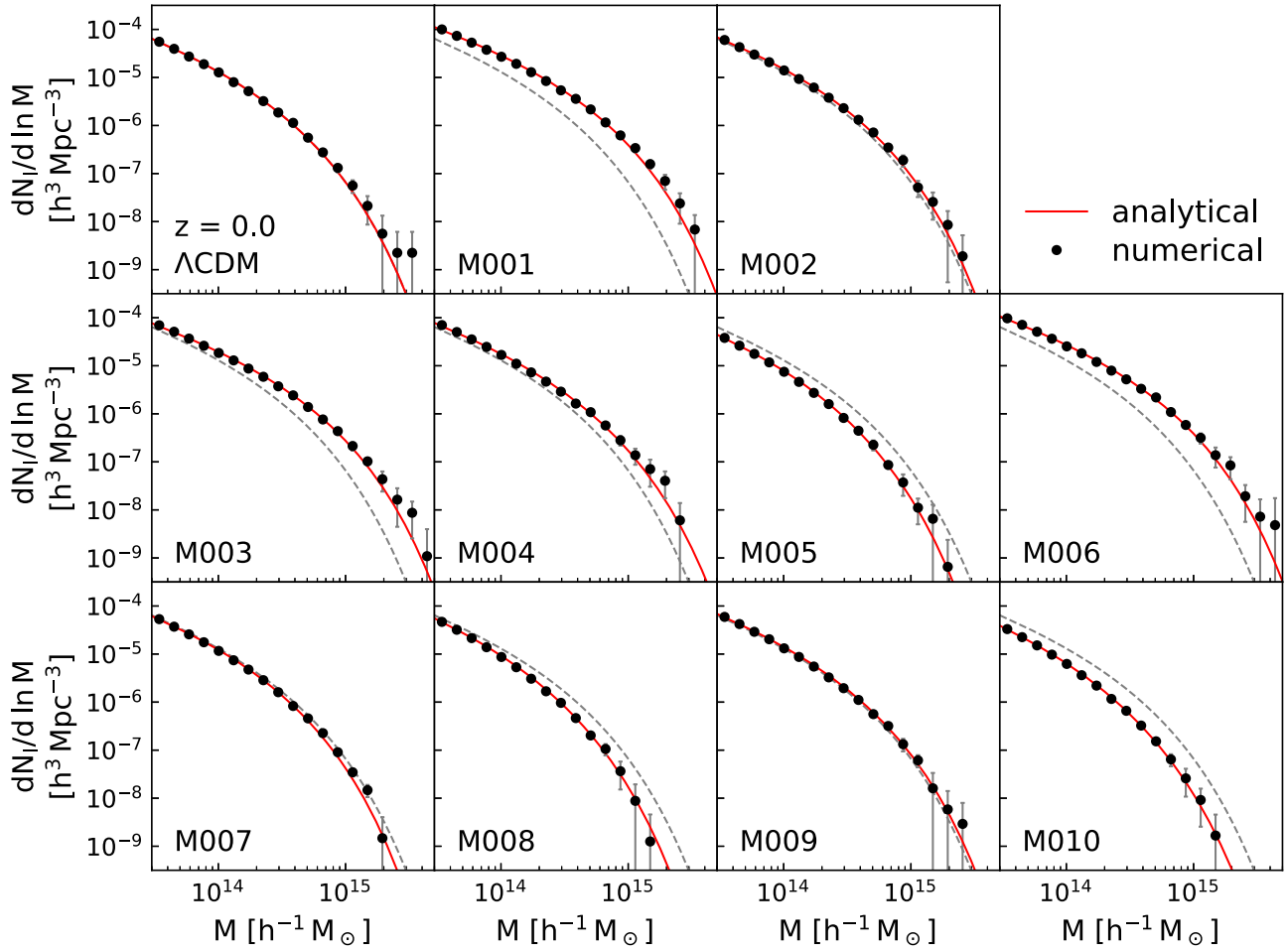

Figure 2. Numerically obtained mass functions of the field clusters (filled circles) compared with the analytic formula (red solid lines) for 10 different dynamical wCDM cosmologies as well as for the ΛCDM case at $z = 0$.

Heitmann et al. (2016) compiled the catalogs of the DM halos identified by applying the friends-of-friends (FoF) algorithm with a linking length of $b_c\bar{d}_p$ with $b_c = 0.168$ and mean particle separation $\bar{d}_p$ to each particle snapshot in the redshift range of $0.0 \leqslant z \leqslant 4.0$. Following the same procedure of Lee (2012), we analyze the FoF halo catalogs from each Mira-Titan universe to numerically determine the mass functions of the field clusters and the associated errors as well.

1. Make a sample of the cluster halos with masses larger than $M_c = 3 \times 10^{13}\, h^{-1} M_\odot$ out of the halo catalog at a given redshift in the range of $0 \leqslant z \leqslant z_c \sim 1$. The catalogs at higher redshifts, $z > z_c$, are excluded from the analysis on the ground that the field clusters at $z > z_c$ are too rare to yield statistically significant results.
2. Apply to the above sample the FoF algorithm with a linking length of $2b_c\bar{d}_c$ with mean cluster halo separation $\bar{d}_c$ to find a supercluster as a cluster of clusters each of which consists of two and more cluster halos. This specific choice of the linking length was made by Lee (2012) to guarantee that the degree of the disturbance from the surroundings on the field clusters is indeed negligible (i.e., $D_B = 0$) (see Figure 2 in Lee 2012).
3. Find the cluster halos in the sample which appertain to none of the identified superclusters as the field clusters and count them, $dN_{\rm I}$, in the logarithmic mass bin, $[\ln M,\ \ln M + d\ln M]$.
4. Split the field clusters into eight Jackknife subsamples according to their positions and separately determine $dN_{\rm I}/d\ln M$ from each subsample. Evaluate the Jackknife errors in the measurement of $dN_{\rm I}/d\ln M$ as one standard deviation scatter around the ensemble average over the eight subsamples.

Now that the mass functions of the field clusters from the Mira-Titan simulations are all determined, we compare them with Equation (8) by adjusting the single coefficient, β. For this comparison, the spherical barrier height, $\delta_{\rm sc}$, is set at the EdS value of 1.686, as it varies only very weakly with the background cosmology (e.g., Eke et al. 1996; Pace et al. 2010). We employ the χ^2-statistics to determine the best-fit value of β and estimate the associated error, σ_β, as $1/\sqrt{I_\beta}$, where I_β is the Fisher information given as $I_\beta \equiv d^2\chi^2/d\beta^2$ at the best-fit value of β, at each redshift for each cosmology.

Figure 2 plots the numerical result (filled circles) as well as Equation (8) with the best-fit value of β (red solid line) for 11 different cosmologies at $z = 0$. In each panel, the analytic mass function with the best-fit β for the ΛCDM case is shown as dotted line for comparison. Figures 3–4 plot the same as Figure 2, but at $z = 0.4$ and $z = 0.78$, respectively. As can be seen, Equation (8) with the best-fit β is quite successful in matching the numerically determined mass functions of the field clusters for all of the 11 cosmologies at all of the three redshifts. As emphasized in Lee (2012), the modified CA

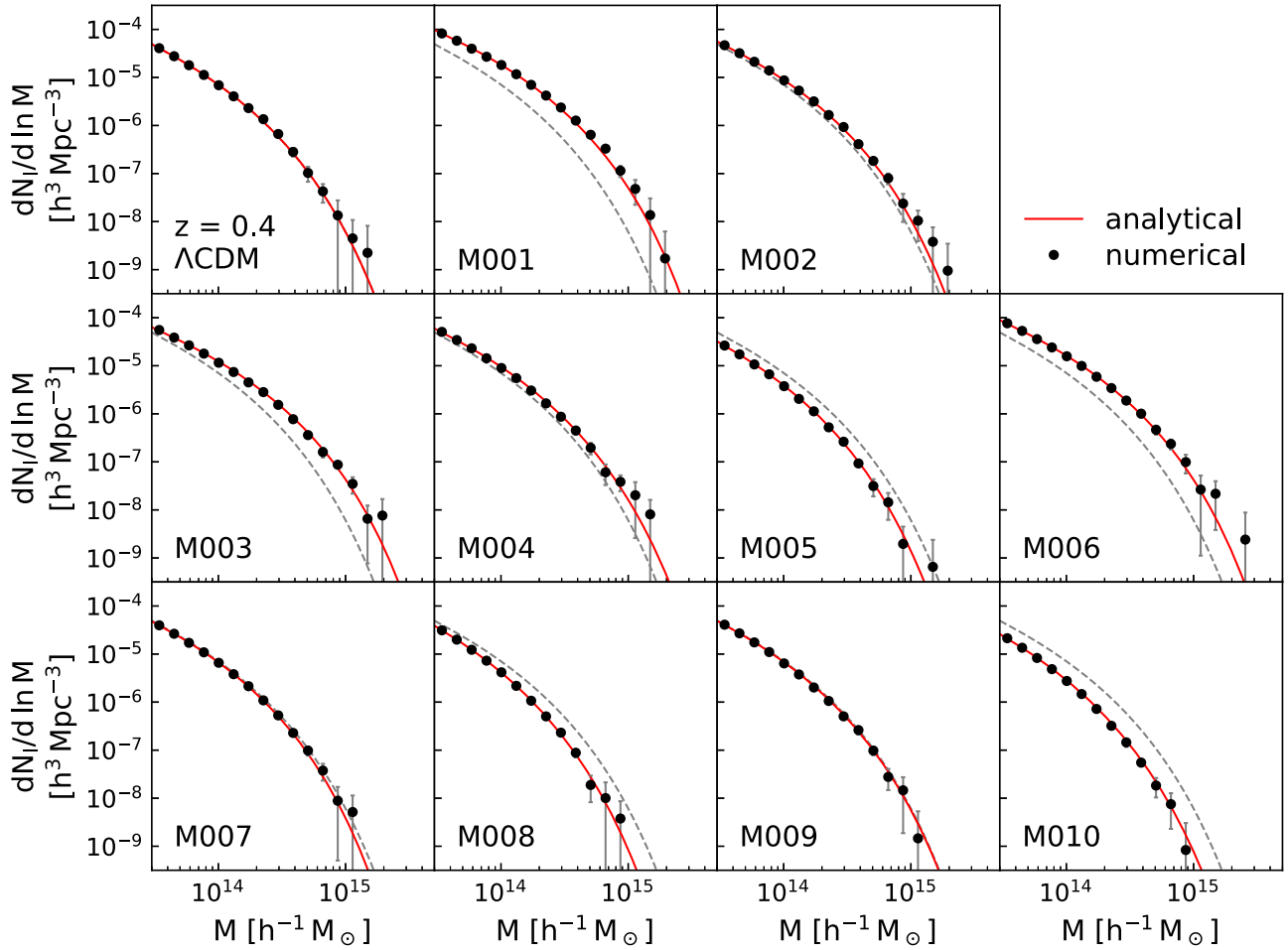

Figure 3. Same as Figure 2, but for at $z = 0.4$.

formalism with $D_B = 0$ describes well not only the shape but also amplitude of the mass function of the field clusters even though it has only a single parameter, β. The good agreements between the analytical and numerical results shown in Figures 2–4 prove that the modified CA formalism with the deterministic collapse barrier for the field clusters can be legitimately extended to the wCDM cosmologies.

It is, however, worth mentioning here that the analytic model for the field cluster mass function, Equation (8), is found to be valid in the limited redshift range $z \leqslant z_c$, which we suspect is due to the failure of the assumption $D_B = 0$ at higher redshifts $z > z_c \sim 1$. The low abundance of the clusters with $M \geqslant M_c$ at $z > z_c$ makes it difficult to properly identify the superclusters via the FoF algorithm, which in turn contaminates the identification of the field clusters. In other words, the field clusters identified via the FoF algorithm at $z > z_c$ may not be isolated enough to satisfy the condition of $D_B = 0$.

2.3. Evolution of the Drifting Collapse Barrier

Figure 5 plots the best-fit value of β determined in Section 2.2 versus z for the 11 cosmologies, revealing the presence of a strong anticorrelation between β and z. We discover an universal behavior of $\beta(z)$ from all of the 11 cosmologies: it monotonically declines toward 0 as the redshift increases up to $z \geqslant 1$. In the range of $0 \leqslant z \leqslant 0.3$, it declines relatively slowly with z, while in the higher z-range it drops quite rapidly down to zero. The drifting coefficient, $\beta(z)$, from each of the 11 cosmologies is, however, manifestly different from one another in its declining rate and amplitude as well as in the critical redshift at which $\beta(z)$ becomes zero.

Although $\delta_{\rm sc}/\sigma(M, z)$ may play a partial role to induce the cosmology dependence of $\beta(z)$, we believe that it should not be the main contribution. First of all, the spherical collapse barrier height, $\delta_{\rm sc}$, has been known to be quite insensitive to the background cosmology as mentioned in Section 2.2. For the case of flat ΛCDM models, Eke et al. (1996) showed that $\delta_{\rm sc}$ changes very mildly from 1.686 to 1.67 as Ω_m changes from 1 to 0.1. Even for the case of flat wCDM models, the weak dependence of $\delta_{\rm sc}$ was rigorously proved by Pace et al. (2010), who directly solved the nonlinear differential equation of the density contrast in the spherical collapse process to find that the value of $\delta_{\rm sc}(z)$ for the wCDM models remain very similar to that for the ΛCDM model in the whole redshift range.

Regarding the cosmology dependence of $\sigma(M, z)$, it depends on the background cosmology only through $D(z)$ and $P(k)$. Whereas, as can be seen in Figure 5, $\beta(z)$ differs even among those models which have the same shapes of $D(z)$ and $P(k)$. Therefore, the cosmology dependence of $\beta(z)$ witnessed in Figure 5 should come mainly from another channel, which we believe is the departure of δ_c from $\delta_{\rm sc}$. In different cosmologies, the nonspherical collapse in the nonlinear regime would proceed differently, resulting in the cosmology dependence of the degree of the departure of δ_c from $\delta_{\rm sc}$, which is described by

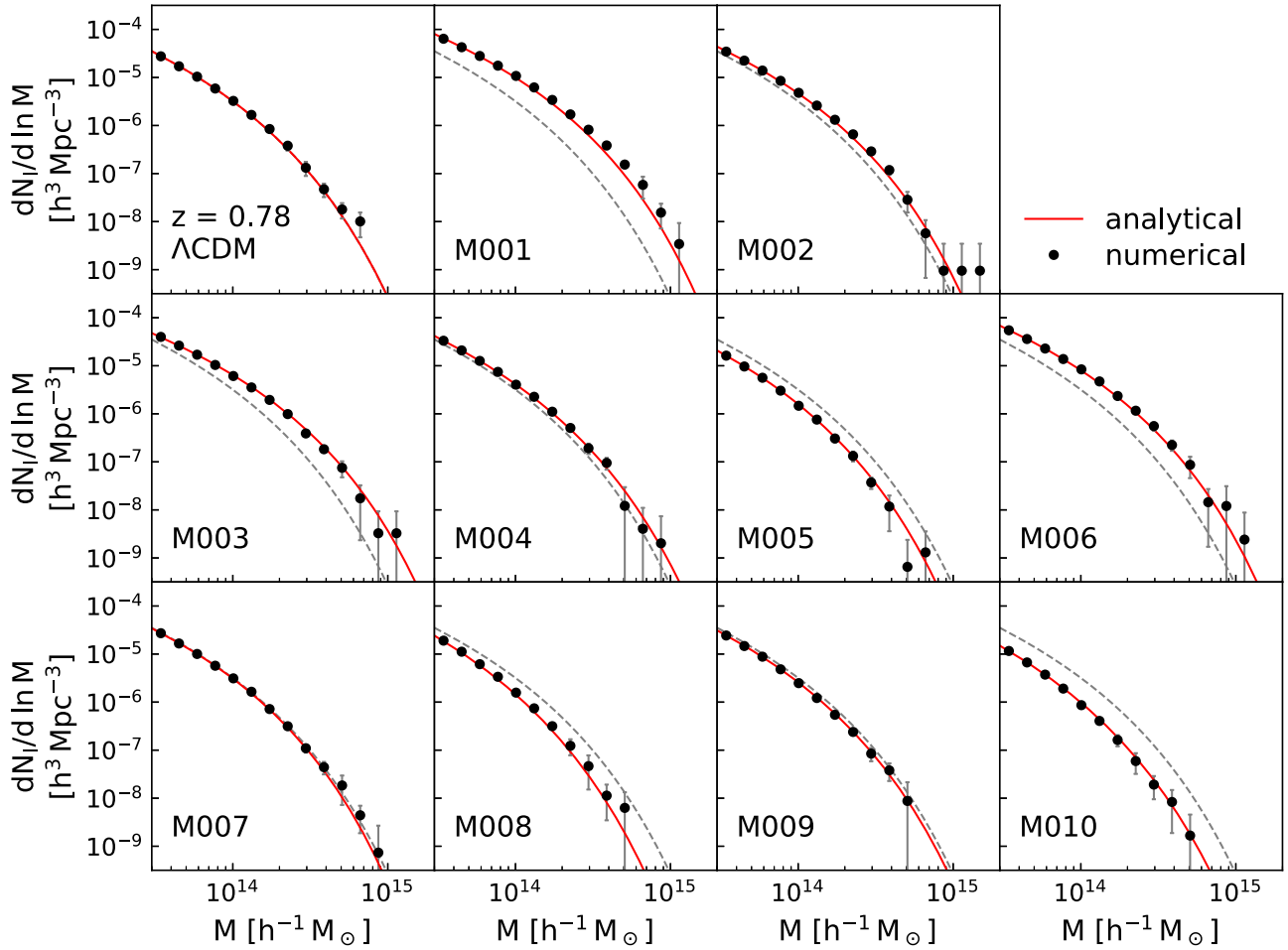

Figure 4. Same as Figure 2, but for at $z = 0.78$.

the single parameter, $\beta(z)$, for the case of the field cluster abundance.

Without having a physical model for the effect of the background cosmology on the departure of δ_c from δ_{sc} at the moment, we find the following fitting formula useful to quantitatively describe the ways in which $\beta(z)$ differs among the 11 cosmologies and to efficiently assess the statistical significances of their differences:

$$\beta(z) = \beta_A \sinh^{-1}\left[\frac{1}{q_z}(z - z_c)\right], \quad (9)$$

where three adjustable parameters, β_A, q_z, and z_c, denote the amplitude, redshift dispersion and critical redshift of $\beta(z)$, respectively. The overall amplitude, β_A, quantifies how much δ_c departs from the EdS value of δ_{sc} at $z = 0$, the critical redshift parameter, z_c, quantifies when δ_c becomes equal to δ_{sc}, while the inverse of the redshift dispersion, $1/q_z$, quantifies the rate at which δ_c converges to δ_{sc}, as z increases. The best-fit values of (β_A, q_z, z_c) and their associated errors $(\sigma_{\beta_A}, \sigma_{q_z}, \sigma_{z_c})$ are obtained by fitting Equation (9) to the empirically determined $\beta(z)$ in Section 2.2 with the help of the ordinary least square code (see Table 2).

Figure 6 shows how well Equation (9) with three best-fit parameters (red solid line) describes the empirically determined $\beta(z)$ (filled circles), comparing the best-fit $\beta(z)$ for each of the 10 wCDM cosmologies with that for the ΛCDM case (dotted line). It is interesting to see that the three cosmologies, ΛCDM, M007, and M009, which produce almost identical mass functions of the field clusters at all redshifts (Figures 2–4), can still be distinguished by their distinct $\beta(z)$. The differences in the best-fit values of the critical redshifts, Δ_{zc}, between the ΛCDM and M007 (M009) cases is as high as $3.47\sigma_{\Delta_{zc}}$ ($5.89\sigma_{\Delta_{zc}}$). Here, the errors, $\sigma_{\Delta_{zc}}$ is calculated through the error propagation as $\sigma_{\Delta_{zc}} \equiv (\sigma^2_{zc,1} + \sigma^2_{zc,2})^{1/2}$ where $\sigma_{zc,1}$ and $\sigma_{zc,2}$ are the errors in the measurements of z_c for the ΛCDM and

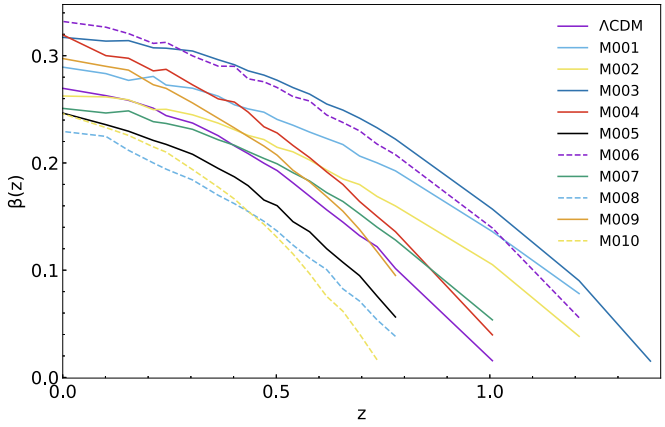

Figure 5. Redshift evolution of the drifting coefficient, β, for 11 different DE cosmologies.

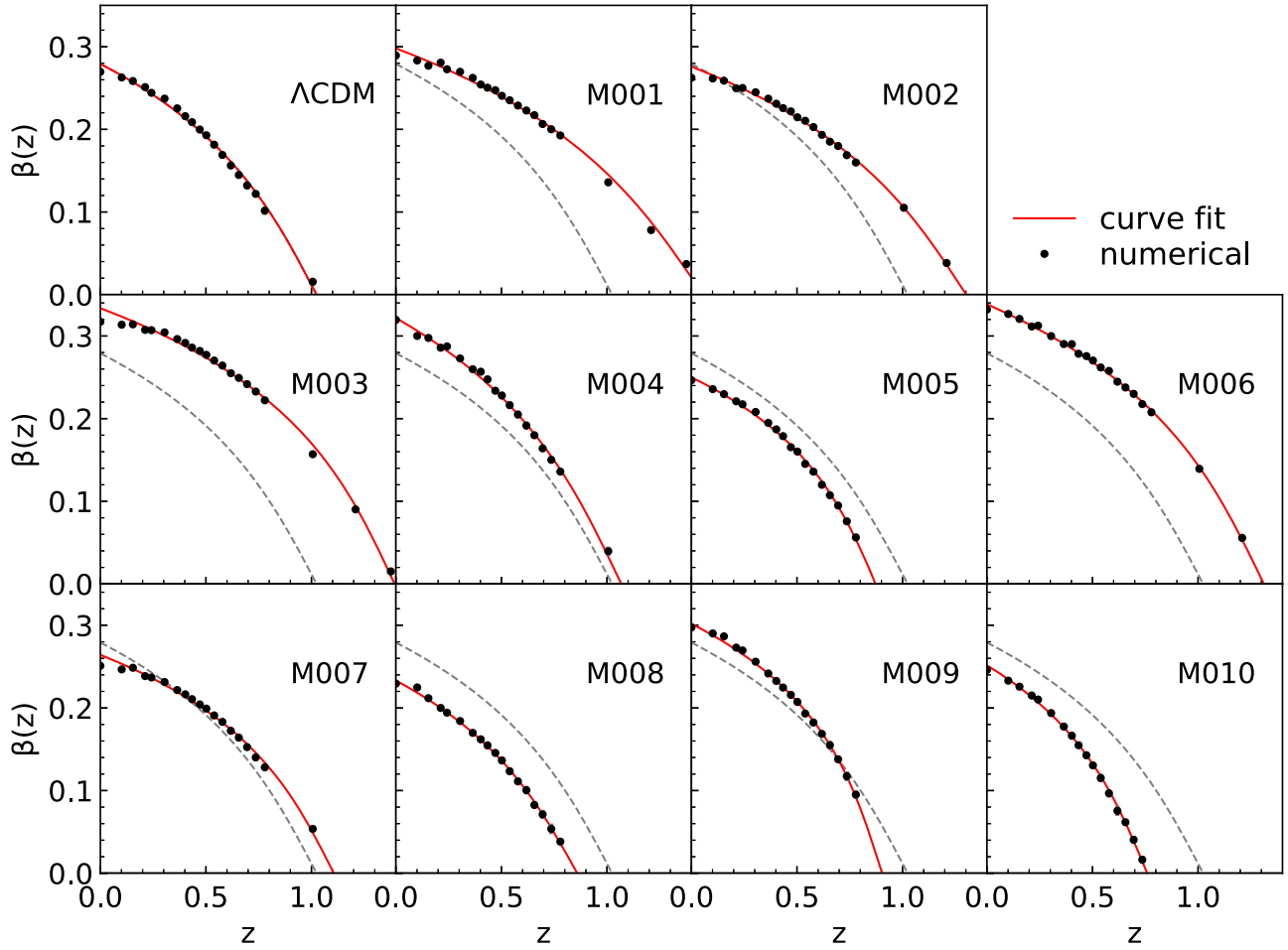

Figure 6. Linear fits (red solid lines) to the numerically obtained $\beta(z)$ (filled circles) for 11 different DE cosmologies.

Table 2
Best-fit Parameters for the Evolution of the Drifting Coefficient

Cosmology	β_A	q_z	z_c
ΛCDM	-0.141 ± 0.008	0.289 ± 0.033	1.024 ± 0.014
M001	-0.147 ± 0.008	0.388 ± 0.045	1.456 ± 0.018
M002	-0.135 ± 0.005	0.343 ± 0.026	1.302 ± 0.014
M003	-0.138 ± 0.006	0.252 ± 0.026	1.394 ± 0.011
M004	-0.163 ± 0.008	0.303 ± 0.032	1.068 ± 0.014
M005	-0.111 ± 0.005	0.186 ± 0.018	0.872 ± 0.009
M006	-0.152 ± 0.005	0.285 ± 0.021	1.311 ± 0.012
M007	-0.116 ± 0.007	0.229 ± 0.031	1.106 ± 0.019
M008	-0.124 ± 0.005	0.269 ± 0.021	0.859 ± 0.007
M009	-0.120 ± 0.006	0.147 ± 0.019	0.903 ± 0.015
M010	-0.123 ± 0.004	0.199 ± 0.013	0.759 ± 0.005

M007 (M009) cases, respectively. Note also that $\beta(z)$ can also distinguish between the two cosmologies, M002 and ΛCDM, although both of the cosmologies yield quite similar linear growth factors and field cluster mass functions (Figure 1). The difference, Δ_{zc}, between the two cosmologies is found to be as significant as $14\sigma_{\Delta_{zc}}$.

The evolution of $\beta(z)$ also allows us to distinguish not only between the wCDM and ΛCDM cosmologies but also among different wCDM cosmologies themselves. For instance, the two wCDM cosmologies, M001 and M006, are found to have almost no difference in their field cluster mass functions. Nevertheless, they can be distinguished by the $6.7\sigma_{\Delta_{zc}}$ differences in the best-fit values of z_c. These results clearly indicates a potential of $\beta(z)$ to complement the cluster mass function in discriminating the candidate cosmologies.

3. Summary and Discussion

Numerically determining the field cluster mass functions at various redshifts from the Mira-Titan simulations for 11 different DE cosmologies (10 different wCDM and one ΛCDM cosmologies) whose key cosmological parameters are chosen to be in the range covering well the *WMAP*7 constraints, we have shown that the numerical results at all redshifts for all 11 cosmologies agree very well with the analytic model obtained by Lee (2012) through a modification of the generalized excursion set formalism (Figures 2–4). The success of the analytic model has validated the key assumptions of Lee (2012) that for the field clusters the collapse barrier can be deemed deterministic and thus that their excursion set mass function can be fully characterized by a single *drifting coefficient*, β, which measures the degree of the departure of the collapse barrier height from the spherical height, $\delta_{\rm sc}$. It has been found that $\beta(z)$ exhibits a universal tendency of converging to zero with the increment of z and that its convergence rate as well as the value of critical redshift, z_c at which $\beta(z) = 0$ depends strongly on the background cosmology (Figure 5). Noting that $\beta(z)$ differs even among those cosmologies that are degenerate with one another in the linear power spectrum, linear growth

factor and cluster mass function, we suggest that $\beta(z)$ should be in principle useful to discriminate the candidate cosmologies.

Nevertheless, as the 11 Mira-Titan cosmologies differ not only in their DE equation of states (w_0, w_a) and DE density parameters ($\Omega_{\rm de}$) but also in the values of the other five key cosmological parameters (h, Ω_m, Ω_b, n_s, σ_8), the detected strong cosmology dependence of $\beta(z)$ cannot be entirely ascribed to the differences among the 11 models in the values of w_0, w_a and $\Omega_{\rm de}$. In other words, our work has demonstrated the usefulness of $\beta(z)$ as a discriminator of wCDM cosmologies from the ΛCDM model, but not as a complementary probe of DE equation of state.

A more comprehensive investigation should be carried out to sort out the sole effect of the DE equation of state on $\beta(z)$ before claiming it as a probe of DE in practice. What will be highly desirable is to examine how sensitively $\beta(z)$ reacts to the variations of the DE equation of state and density parameter by determining its shapes from a series of N-body simulations each of which has a different DE equation of state but the same values of the other key cosmological parameters. What will be even more highly desirable is to construct a theoretical formula for $\beta(z)$ from a physical principle. Although Equation (9) is a mere fitting formula expressed in terms of an inverse sine hyperbolic function with three adjustable parameters, its general success in matching $\beta(z)$ for all of the 11 cosmologies (Figure 6) hints a prospect for finding a physical formula similar to it and directly linking its three parameters to the initial conditions. This physical formula, if found and verified to be robust, would allow us to probe not only the DE equation of state and density parameter but also the other alternative cosmologies such massive neutrinos, modified gravity and etc, with $\beta(z)$. Our future work is in this direction.

We thank the anonymous referee for very useful comments which helped us improve the original manuscript. We acknowledge the support by Basic Science Research Program through the National Research Foundation (NRF) of Korea funded by the Ministry of Education (No. 2019R1A2C1083855) and also by a research grant from the NRF to the Center for Galaxy Evolution Research (No. 2017R1A5A1070354).

An award of computer time was provided by the Innovative and Novel Computational Impact on Theory and Experiment (INCITE) program. This research used resources of the Argonne Leadership Computing Facility, which is a DOE Office of Science User Facility supported under contract DE-AC02-06CH11357. This research also used resources of the Oak Ridge Leadership Computing Facility, which is a DOE Office of Science User Facility supported under Contract DE-AC05-00OR22725.

ORCID iDs

Jounghun Lee https://orcid.org/0000-0003-0522-4356

References

Achitouv, I., Wagner, C., Weller, J., et al. 2014, JCAP, 2014, 077
Basilakos, S., Plionis, M., & Lima, J. A. S. 2010, PhRvD, 82, 083517
Benson, B. A., de Haan, T., Dudley, J. P., et al. 2013, ApJ, 763, 147
Bernardeau, F. 1994, ApJ, 427, 51
Bond, J. R., & Myers, S. T. 1996, ApJS, 103, 1
Chevallier, M., & Polarski, D. 2001, IJMPD, 10, 213
Chiueh, T., & Lee, J. 2001, ApJ, 555, 83
Corasaniti, P. S., & Achitouv, I. 2011a, PhRvL, 106, 241302
Corasaniti, P. S., & Achitouv, I. 2011b, PhRvD, 84, 023009
Eke, V. R., Cole, S., & Frenk, C. S. 1996, MNRAS, 282, 263
Fan, X., Bahcall, N. A., & Cen, R. 1997, ApJL, 490, L123
Gunn, J. E., & Gott, J. R. 1972, ApJ, 176, 1
Habib, S., Pope, A., Finkel, H., et al. 2016, NewA, 42, 49
Heitmann, K., Bingham, D., Lawrence, E., et al. 2016, ApJ, 820, 108
Heitmann, K., Higdon, D., White, M., et al. 2009, ApJ, 705, 156
Heitmann, K., Uram, T. D., Finkel, H., et al. 2019, ApJS, 244, 17
Ichiki, K., & Takada, M. 2012, PhRvD, 85, 063521
Komatsu, E., Smith, K. M., Dunkley, J., et al. 2011, ApJS, 192, 18
Lawrence, E., Heitmann, K., Kwan, J., et al. 2017, ApJ, 847, 50
Lee, J. 2012, ApJ, 752, 40
Lewis, A., Challinor, A., & Lasenby, A. 2000, ApJ, 538, 473
Linder, E. V. 2003, PhRvL, 90, 091301
Maggiore, M., & Riotto, A. 2010a, ApJ, 711, 907
Maggiore, M., & Riotto, A. 2010b, ApJ, 717, 515
Pace, F., Waizmann, J. C., & Bartelmann, M. 2010, MNRAS, 406, 1865
Planck Collaboration, Ade, P. A. R., Aghanim, N., et al. 2014, A&A, 571, A20
Press, W. H., & Schechter, P. 1974, ApJ, 187, 425
Reed, D., Gardner, J., Quinn, T., et al. 2003, MNRAS, 346, 565
Robertson, B. E., Kravtsov, A. V., Tinker, J., et al. 2009, ApJ, 696, 636
Sheth, R. K., Mo, H. J., & Tormen, G. 2001, MNRAS, 323, 1
Sheth, R. K., & Tormen, G. 2002, MNRAS, 329, 61
Tinker, J., Kravtsov, A. V., Klypin, A., et al. 2008, ApJ, 688, 709
Vikhlinin, A., Kravtsov, A. V., Burenin, R. A., et al. 2009, ApJ, 692, 1060
Wang, L., & Steinhardt, P. J. 1998, ApJ, 508, 483